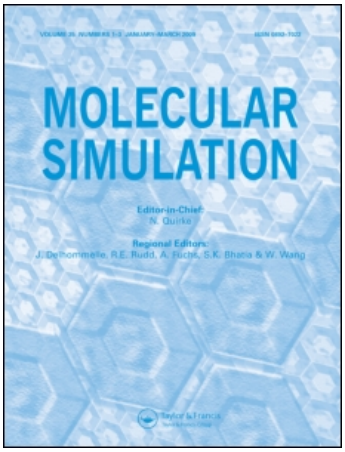

Molecular Simulation

Publication details, including instructions for authors and subscription information:
http://www.informaworld.com/smpp/title~content=t713644482

Molecular dynamics study of carbon nanotube oscillator on gold surface

J. W. Kang[a]; O. K. Kwon[b]; J. H. Lee[c]; Q. Jiang[a]; H. J. Hwang[d]

[a] Department of Mechanical Engineering, University of California, Riverside, CA, USA [b] Department of Internet Information, Semyung University, Jecheon, Republic of Korea [c] Information Display Research Center and Department of Computer System Engineering, Sangmyung University, Chonan, Republic of Korea [d] School of Electrical and Electronic Engineering, Chung-Ang University, Seoul, Republic of Korea

To cite this Article Kang, J. W. , Kwon, O. K. , Lee, J. H. , Jiang, Q. and Hwang, H. J.(2006) 'Molecular dynamics study of carbon nanotube oscillator on gold surface', Molecular Simulation, 32: 5, 363 — 368

To link to this Article: DOI: 10.1080/08927020600755145

URL: http://dx.doi.org/10.1080/08927020600755145

Molecular Simulation, Vol. 32, No. 5, 30 April 2006, 363–368

Taylor & Francis
Taylor & Francis Group

Molecular dynamics study of carbon nanotube oscillator on gold surface

J. W. KANG†‡, O. K. KWON¶, J. H. LEE§, Q. JIANG‡ and H. J. HWANG*†

†School of Electrical and Electronic Engineering, Chung-Ang University, 221 HukSuk-Dong, DongJak-Ku, Seoul 156-756, Republic of Korea
‡Department of Mechanical Engineering, University of California, Riverside, CA 92521, USA
¶Department of Internet Information, Semyung University, Jecheon 390-711, Republic of Korea
§Information Display Research Center and Department of Computer System Engineering, Sangmyung University, Chonan 330-720, Republic of Korea

(Received January 2006; in final form March 2006)

We investigated the substrate effect of carbon nanotube (CNT) oscillators using classical molecular dynamics simulations. Double-walled CNT oscillators on {100} gold surface were considered. The nanotube–gold interactions induced the compressive deformations of the outer nanotube and affected the transitional velocity and the energy dissipation of the nanotube oscillator. When the inner nanotube was extruded from the outer nanotube, the central regions of the outer nanotube were compressed by the nanotube–gold interactions and then, these compressive forces pushed out the inner nanotube and finally, the transitional velocity of the inner nanotube was slightly increased at the edges regions. Since the energy dissipation of the nanotube oscillator on gold surface was higher than that in vapor, the decrease of the transitional velocity for the nanotube oscillator on gold surface was greater than that for the nanotube oscillator in vapor.

Keywords: Nanotube oscillator; Molecular dynamics; Carbon nanotube; Deformations

PACS numbers: 61.46.+w; 66.30.Pa; 83.10.Rs

1. Introduction

Cumings and Zettl [1] reported an ideal low-friction and low-wear bearing carved out of a multi-walled carbon nanotube (CNT) with diameter of a few tens of nanometers. Gigahertz CNT-based oscillators have been suggested by Zheng and Jiang [2]. The tools of molecular dynamics (MD) can in principle be employed to predict the performance of nanoscale machine components. CNT oscillators based on multi-walled CNTs have been widely investigated using the MD simulations [3–20]. Zheng *et al.* [3] have investigated the detailed theoretical calculations of the excess van der Waals (vdW) energy due to the extrusion and the corresponding restoring force. Energy dissipations of CNT oscillators have been investigated from Guo *et al.* [4], Jiang *et al.* [5,6] and Tangney *et al.* [7]. Legoas *et al.* [8,9] have presented the MD simulations for these systems, which considered the different nanotube types in order to verify the reliability of such devices as gigahertz oscillators. They showed that these nano-oscillators are dynamically stable when the radii difference values between inner and outer tube are of ~3.4 Å. Rivera *et al.* [10] investigated the oscillatory damped behavior of the incommensurate double-walled CNTs. Gigahertz oscillations of multi-walled CNT oscillators have been investigated by classical MD simulations [11,16]. Coluci *et al.* [12] showed chaotic signature in the motion of coupled CNT oscillators. Liu *et al.* [13] investigated the mechanism leading to unstable oscillatory behavior of double-walled CNT oscillators by five different vdW potentials. Triple-walled CNT oscillators have been investigated by classical MD simulations [6,12].

Until now, gigahertz multi-walled CNT-based oscillators in vapor have been investigated [2–20]. However, most nanodevices based on nanotubes have been realized on substrates supporting the nanotubes. The vdW interactions between the nanotube and the substrate cause a deformation of the nanotube [21,22]. The cross-sectional deformation induced by the vdW forces between the nanotube and the substrate is much higher in single-walled CNTs than in multi-walled nanotubes [21,22].

*Corresponding author. Tel: 82-2-820-5296. Fax: 82-2-825-1584/82-2-812-5318. Email: hjhwang@cau.ac.kr

Molecular Simulation
ISSN 0892-7022 print/ISSN 1029-0435 online © 2006 Taylor & Francis
http://www.tandf.co.uk/journals
DOI: 10.1080/08927020600755145

The vdW forces between the nanotube and the substrate can also affect the operation of the fullerene-shuttle memory devices [23,24]. CNT oscillators can be fabricated and operated on substrates. However, the effects of the vdW forces for the CNT-based oscillators have never been investigated in previous works. Therefore, in this work, the nanotube-substrate interaction effect for the CNT-based oscillator was investigated using classical MD simulations. In this paper, our MD simulation results for double-walled CNT oscillators on gold surface show that the vdW interactions between the CNT and the substrate induce the compressive deformations of the CNT; then, the frictional forces are increased and affect the frequency, the shuttle CNT velocity and the damping rate of their operations.

2. Methods

For carbon–carbon interactions, we used the Tersoff–Brenner potential function that has been widely applied to carbon systems [25–27]. For carbon–carbon vdW interactions, we used a Lennard–Jones (LJ12-6) potential function [28] with parameters $\sigma = 3.4$ Å and $\varepsilon = 0.0024$ eV, and the cutoff distance was taken to be 20 Å. In this wok, we considered the gold as the substrate. For the gold–gold and the gold–carbon interaction, we employed the Lennard–Jones 12–6 potential function with parameters. The values of σ_{AuC} and ε_{AuC} for the LJ12–6 potential for gold–carbon are 2.9943 Å and 0.01273 eV, respectively [29]. The values of σ_{Au} and ε_{Au} for the LJ12–6 potential for gold are 2.569 Å and 0.458 eV, respectively [30].

We used both the steepest descent (SD) and the MD methods. The MD simulations used the same MD methods as used in our previous works [31–35]. The MD code used the velocity Verlet algorithm, a Gunsteren–Berendsen thermostat to control temperature, and neighbor lists to improve computing performance. MD time step (Δt) was 5×10^{-4} ps. Firstly, all structures were relaxed by SD simulations. The initial temperatures of all MD simulations have been set at 1 K, and the total energy was constantly maintained during all MD simulations.

Figure 1 shows simple schematics of simulation structures. We considered two CNT-based oscillators composed of (5,5)–(10,10) double-walled CNTs. Short CNT oscillator was composed of the length of 30 Å for both outer and inner CNTs, and both CNTs had a open ends. Long CNT oscillator was composed of the opened (10,10) CNT with the length of 116 Å and the capped (5,5) CNT with the length of 32 Å. Substrate was composed of five atomic layers of {100} gold surface with the width of 34 Å, and the lengths of the substrate 34 and 120 Å for the short and the long CNTs, respectively. The lengths of the gold substrates were the same as the CNT lengths, such as CNT oscillator schematics addressed in our previous work [20]. The bottom and the side layers of the substrate were fixed and the constraint dynamics were applied to the other atoms. In figure 1, P_{outer} and P_{inner} indicate the central positions of the outer and inner CNTs, and d_{re} is the distance between P_{outer} and P_{inner}. The inner CNT oscillator was initiated by an initial velocity, v_T, or an initial displacement. The CNT oscillators supported by gold surface were compared to the CNT oscillator in vapor.

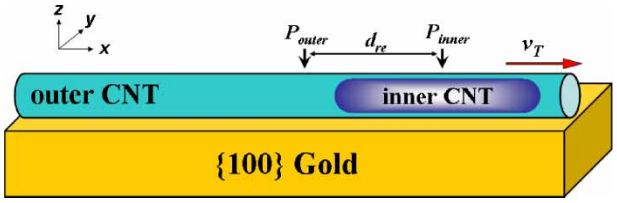

Figure 1. Simple schematics of simulation structures. P_{outer} and P_{inner} indicate the central positions of the outer and inner CNTs, and d_{re} is the distance between P_{outer} and P_{inner}. v_T is initial transitional velocity of the inner CNT.

3. Results and discussion

Figure 2 shows MD simulation results for the short CNT oscillator, when the inner CNT was initially displacement by 15 Å as shown in figure 2(b). The solid and the symbol

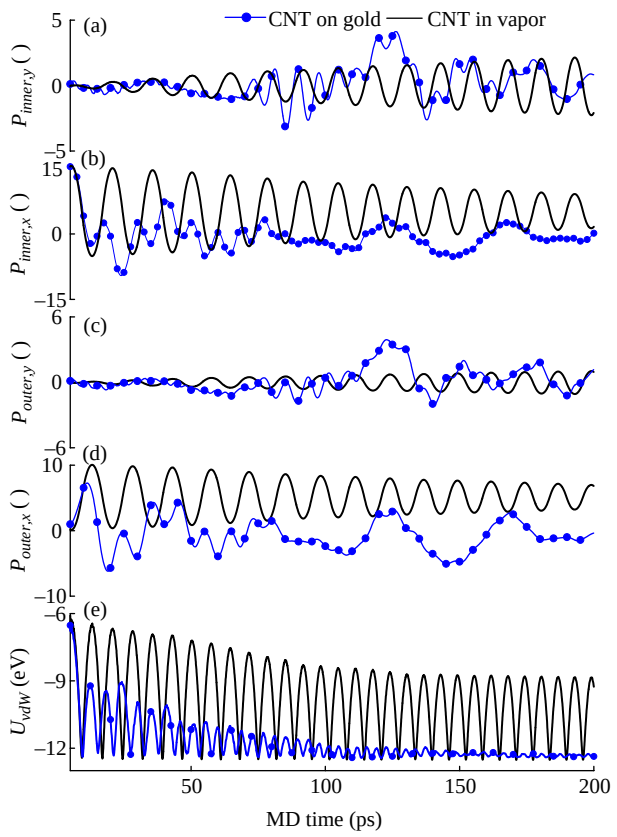

Figure 2. MD simulation results for the short CNT oscillator. The inner CNT was initially displacement by 15 Å. The solid and the symbol lines indicate the results of the CNTs on gold surface and in vapor, respectively. (a) x and (b) y components of P_{inner}, (c) x and (d) y components of P_{outer}, and (e) the vdW energy (U_{vdW}).

lines indicate the results of the CNTs on gold and in vapor, respectively. Since the forces between the outer and the inner CNTs were attractive, both the outer and the inner CNT moved toward each other found in figure 2(b),(d). Therefore, both CNTs showed the transitional motions. For the CNT oscillator in vapor, the regular oscillations were found and the peaks were gradually decreased by the energy dissipation, i.e. the transitional kinetic energies of both CNTs were changed to thermal energies of themselves by the frictional forces between the walls. As shown in figure 2(a),(c), the transitional energy of the CNT oscillator was also transferred into the rotational energy of the CNT oscillator on the gold surface. CNT oscillator moved to possess the largest contact area between the CNT and the gold surface, and this was the origin of the torque on the short CNT oscillator in our MD simulations. However, for the long CNT oscillator, its rotational motion was insignificant. The energy dissipation of the CNT oscillator in vapor can be also found in the vdW energy variation (U_{vdW}) of figure 2(e). The oscillation feature of the CNT oscillator on gold was greatly different from that of the CNT oscillator in vapor. Since the outer CNT interacted with the gold surface, the behavior of the outer CNT on gold was different from that in vapor as shown in figure 2(d). The oscillatory behavior of the CNT oscillator on gold was greatly different from that of the CNT oscillator in vapor, and the energy dissipation of the CNT oscillator on gold was very higher than that of the CNT oscillator in vapor. The oscillations of the CNT oscillator on gold surface were irregular due to the CNT–gold interactions. These results can be also found in figure 2(e). The vdW energy of the CNT oscillator on gold was very rapidly damped.

For the CNT oscillator in vapor, most important energy dissipation mechanism has been found wagging motions of the CNT oscillators at the edge of the outer CNT [5,7,16,17]. The transitional kinetic energies of the CNT oscillators were also dissipated by the friction force, which is induced by the rocking motion of the CNT oscillator during the transitional motion of the CNT oscillator [5,7,17]. For the CNT oscillator with a short outer CNT, the wagging motion of the CNT oscillator at the edge of the outer CNT was most important energy dissipation mechanism. For the CNT oscillator with a long outer CNT, the energy was mainly dissipated by the friction force induced by the vibrational breathing modes of the outer CNT during the transitional motion of the CNT oscillator [5].

In the results of MD simulations, the energy dissipation mechanism for the short CNT oscillator on gold was the wagging motions of the CNT oscillators at the edge of the outer CNT. The wagging motions of the CNT oscillators on gold were higher than those of the CNT oscillators in vapor, because the both edges of the outer CNT were more deformed than the central region of the outer CNT by the CNT–gold interactions. Figure 3 shows the atomic structures at 24 and 42 ps. When the inner CNT was extruded from one side of the outer CNT, the other side of the outer CNT was flattened by the attractive forces between the CNT and the gold surface; then, the extrusion direction of the inner CNT tended the upper side as shown in figure 3. Therefore, the wagging motions of the inner CNT were main mechanism of the energy dissipation for the short CNT oscillator.

We performed the MD simulations for the CNT oscillator with the length of 116 Å including the capped

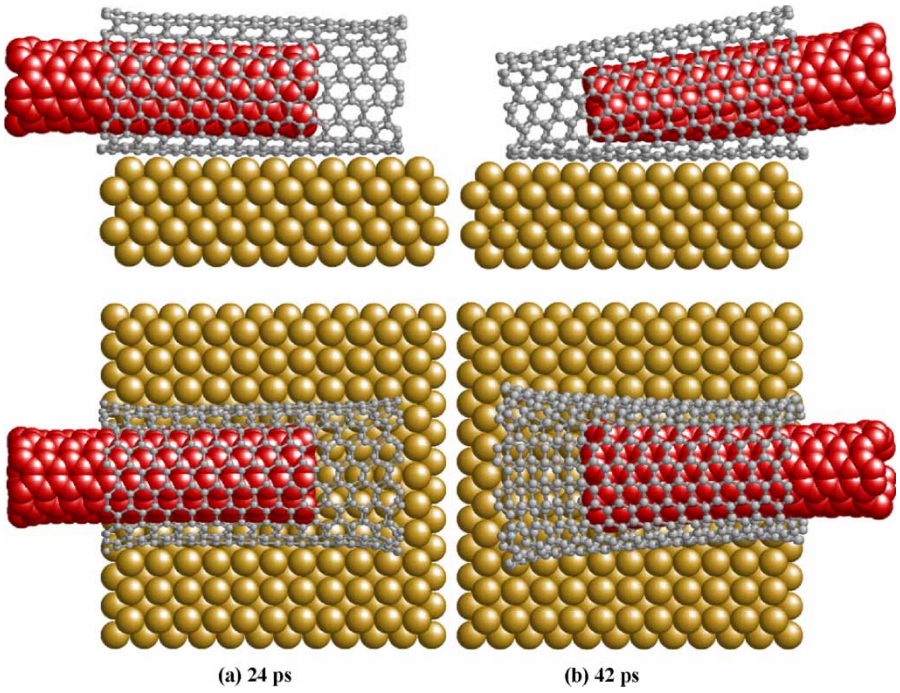

Figure 3. Side and top views of atomic structures at (a) 24 ps and (b) 42 ps.

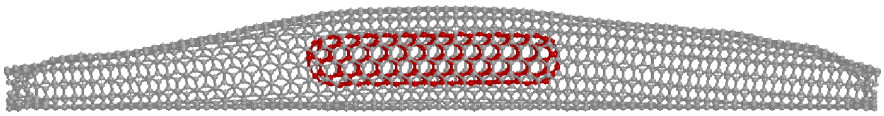

Figure 4. Atomic structure at 10 K obtained from the SA simulation.

(5,5) CNT of 32 Å. After the relaxations by the SD or MD simulations at 1 K, the both ends of the outer (10,10) CNT on gold surface were still opened. However, after a simulated annealing (SA) from 500 K, the both ends were closed by the CNT–gold interactions as shown in figure 4. Figure 4 shows the atomic structure at 10 K during the SA simulation. For MD simulations with initial temperatures of above 100 K, the oscillatory behaviors were not found in the CNT oscillator on gold surface, because the friction forces were very high at the end of the outer CNT or the ends of the outer CNT were closed due to the CNT–gold interaction. Therefore, long CNT oscillator can be formed and operated at very low temperature.

Legoas *et al.* [8] showed that external multi-walled CNT made the more internal shells stiffer as the number of shells increased. Therefore, the edge distortions of the external shells can be reduced, and then, the use of the multi-walled structures could reduce these perturbations. However, in studies by Legoas *et al* [8,9], since the central positions of the external shells were fixed during the core CNT oscillates, the oscillations of some external shells were not achieved. MD simulations of triple-walled CNT oscillators showed that the oscillations of the second shell as well as the core shell were found [6]. Therefore, some external shells of multi-walled CNT oscillators can be influenced on the substrate when they are extruded, the edge distortions of the external shells can be achieved by the substrate–CNT interactions. As the number of shells increases, these effects can be also decreased. To avoid the substrate–induced deformation of the CNT oscillator, the sealing technique proposed by Legoas *et al.* [8,9] could be applied.

Figure 5 shows the MD simulations results of the CNT oscillators with long outer CNT on gold surface and in vapor at 1 K, respectively. The inner CNT was initially positioned at the center of the outer CNT and the initial velocity (v_0) of the inner CNT was 5 Å/ps. Figure 5(a)–(d) shows the relative transitional velocity of the inner CNT (v_T), the relative position of the inner CNT from the center of the outer CNT (d_{re}), the covalent bonding energy of the CNT oscillator (U_{bond}), and the vdW energy (U_{vdW}), respectively. For the CNT oscillator on gold surface, the transitional velocity of the inner CNT was gradually decreased by both the friction force during the transitional motion and the energy dissipations at the both edges of the outer CNT discussed above, and then, v_T of the CNT oscillator on gold surface was less than v_T of the CNT oscillator in vapor. Therefore, the frequency of the CNT oscillator on gold surface was less than that of the CNT oscillator in vapor. As well as the energy dissipation mechanism, v_T variations of the CNT oscillator on gold surface were different from those in vapor. For the CNT oscillator on gold surface, both U_{bond} and U_{vdW} increased when the inner CNT was extruded from the outer CNT, whereas U_{bond} for the CNT oscillator in vapor constantly maintained.

The variation of the transitional velocity (v_T) was investigated as a function of d_{re}. Figure 6(a),(b) shows the v_T–d_{re} plots for the CNT oscillators on gold surface at 1 K with $v_0 = 5$ and 6 Å/ps, respectively. Figure 6(c),(d) shows the v_T–d_{re} plots for the CNT oscillators in vapor at 1 K with $v_0 = 5$ and 6 Å/ps, respectively. For the CNT oscillators in vapor, v_T of the inner CNT was almost continually decreased during the oscillations. For the CNT oscillator in gold surface, v_T slightly increased at both CNT ends and was decreased during the suction into the outer CNT and the transitional motion in the outer CNT. The damping rate of the CNT oscillator on gold surface was five time higher than that of the CNT oscillator in vapor. Thus unique feature of v_T variations for the CNT oscillator on gold surface can be explained by figure 7 that shows the atomic structures at 13.5, 26.0 and 38.0 ps when $v_0 = 5$ Å/ps. When the inner CNT was extruded from the outer CNT as shown in figure 7(a),(c), the central regions of the outer CNT was compressed by the CNT–gold interactions and then, this compressive force as indicated the arrows pushed out the inner CNT. Therefore, the transitional velocity of the inner CNT was increased at

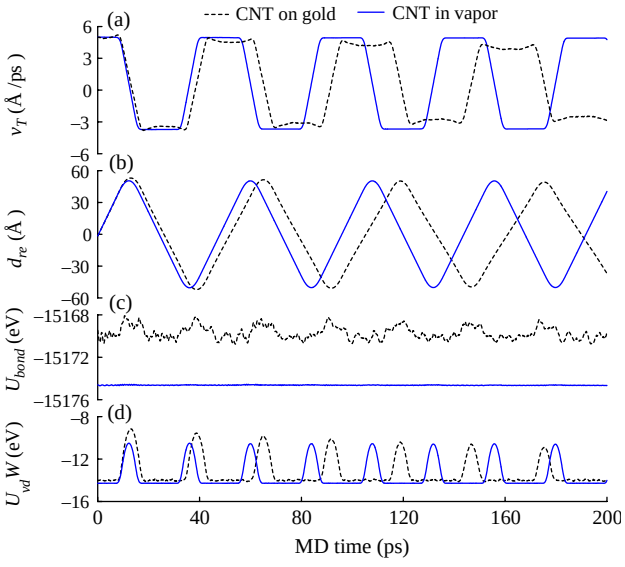

Figure 5. MD simulations results of the CNT oscillators on gold surface and in vapor at 1 K, respectively. The inner CNT was initially positioned at the center of the outer CNT and the initial velocity (v_0) of the inner CNT was 5 Å/ps. (a) The relative transitional velocity of the inner CNT (v_T), (b) the relative position of the inner CNT from the center of the outer CNT (d_{re}), (c) the covalent bonding energy of the CNT oscillator (U_{bond}), and (d) the vdW energy (U_{vdW}), respectively.

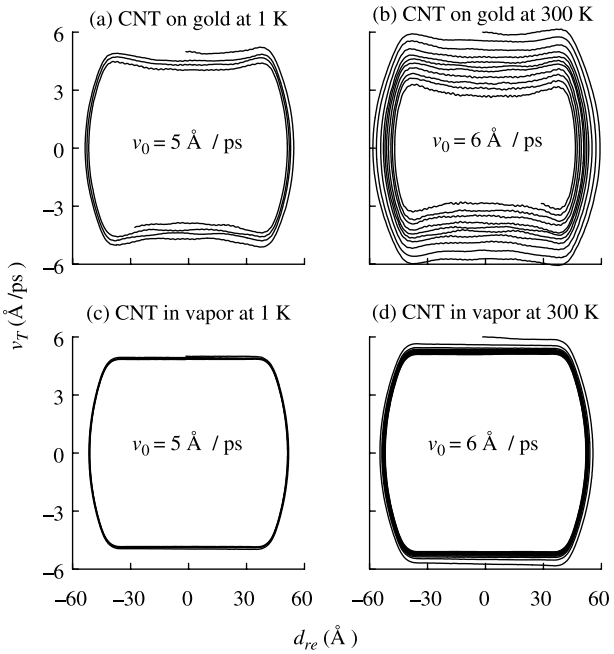

Figure 6. (a) and (b) show the v_T–d_{re} plots for the CNT oscillators on gold surface at 1 K with $v_0 = 5$ and 6 Å/ps, respectively, (c) and (d) show the v_T–d_{re} plots for the CNT oscillators in vapor at 1 K with $v_0 = 5$ and 6 Å/ps, respectively.

the edges. When the inner CNT was positioned inside the outer CNT as shown in figure 7(b), the outer CNT compressed the inner CNT. Therefore, the transitional velocity of the inner CNT was influenced on the surface waves of the outer CNT, and this effect can be found by small ripples in figure 6. These features of the CNT oscillator on gold surface were very similar to the substrate effects for the fullerene-shuttle-memory devices [23]. For the CNT oscillator with a long outer CNT in vapor, the energy was mainly dissipated by the friction force induced by the vibrational breathing modes of the outer CNT during the transitional motion of the CNT oscillator [5]. Thus energy dissipation is greatly influenced on the temperature closely related to breathing of the CNT. As the temperature increases, the effects of both the wagging motion of the CNT oscillator at the edges and the rocking motion of the CNT oscillator during transitional motion also increase. However, since the CNT oscillator on gold surface can be operated by very low temperature as discussed above, the energy is slightly dissipated by the friction force induced by the vibrational breathing modes of the outer CNT during the transitional motion of the CNT oscillator, whereas the energy is mainly dissipated at both edges.

In this work, we considered only {100} gold substrate, which had the same as the length of the CNT oscillators. The operations of the CNT oscillators can be influenced on the substrate dimension. Since the crystallography of the substrate can affect the operations of the CNT oscillators, these effects should be investigated by the further works. When some carbon atoms of the CNT oscillator form the covalent bonds with the substrate, the crystallography of the substrate greatly affect the operation of the CNT oscillator. However, when the CNT–substrate interactions are only non-bond interactions, the deformation of the CNT oscillator is irregardless with the crystallography of the substrate. Therefore, the substrate induced CNT oscillator deformations should be studied in detail. The charge transfers of metal–CNT contacts have been an important issue [36]. The effective charges and the polarization of the CNT oscillator can affect both its operation frequency and frictional force [20]. The charge transfer between the CNT and the substrate should be also considered in the further work. The dynamics behaviors of the CNT oscillators including the charge transfer effect should be studied by MD simulations based on full quantum method.

4. Summary

For the CNT-based oscillators supported by the substrate, the CNT–substrate interaction effect was investigated using classical MD simulations. MD simulation results for double-walled CNT oscillators on gold surface showed that the CNT–gold interactions induced the compressive deformations of the outer CNT and affected the transitional velocity and the energy dissipation of the CNT oscillator. The decrease of the transitional velocity for the CNT oscillator on gold surface was greater than

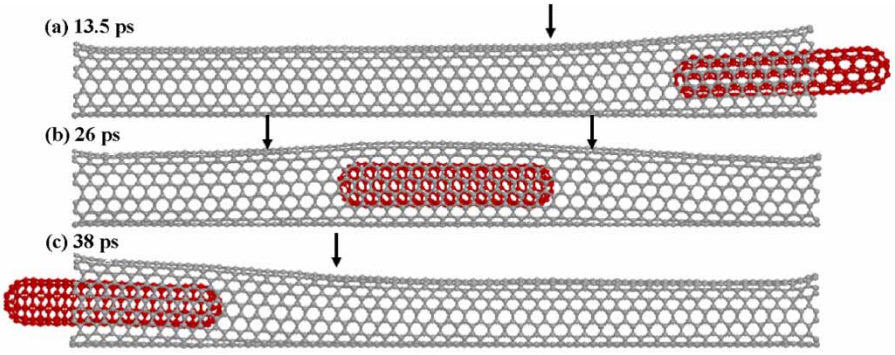

Figure 7. Atomic structures at (a) 13.5, (b) 26.0, and (c) 38.0 ps when $v_0 = 5$ Å/ps.

that for the CNT oscillator in vapor and the frequency of the CNT oscillator on gold surface was less than that of the CNT oscillator in vapor. The CNT oscillator on gold surface could be operated by very low temperature. The energy was mainly dissipated at both edges and the energy dissipation of the CNT oscillator on gold surface was higher than that in vapor. When the inner CNT was extruded from the outer CNT, the central regions of the outer CNT were compressed by the CNT−gold interactions and then, these compressive forces pushed out the inner CNT and finally, the transitional velocity of the inner CNT was slightly increased at the edges.

References

[1] J. Cumings, A. Zettl. Low-friction nanoscale linear bearing realized from multiwall carbon nanotubes. *Science*, **289**, 602 (2000).

[2] Q. Zheng, Q. Jiang. Multiwalled carbon nanotubes as gigahertz oscillators. *Phys. Rev. Lett.*, **88**, 045503 (2002).

[3] Q. Zheng, J.S. Liu, Q. Jiang. Excess van der Waals interaction energy of a multiwalled carbon nanotube with an extruded core and the induced core oscillation. *Phys. Rev. B*, **65**, 245409 (2002).

[4] W. Guo, Y. Guo, H. Gao, Q. Zheng, W. Zheng. Energy dissipation in gigahertz oscillators from multiwalled carbon nanotubes. *Phys. Rev. Lett.*, **91**, 125501 (2003).

[5] Y. Zhao, C-C. Ma, G. Chen, Q. Jiang. Energy dissipation mechanisms in carbon nanotube oscillators. *Phys. Rev. Lett.*, **91**, 175504 (2003).

[6] C-C. Ma, Y. Zhao, C-Y. Yam, G.H. Chen, Q. Jiang. A tribological study of double-walled and triple-walled carbon nanotube oscillators. *Nanotechnology*, **16**, 1253 (2005).

[7] P. Tangney, S.G. Louie, M.L. Cohen. Dynamic sliding friction between concentric carbon nanotubes. *Phys. Rev. Lett.*, **93**, 065503 (2004).

[8] S.B. Legoas, V.R. Coluci, S.F. Braga, P.Z. Coura, S.O. Dantas, D.S. Galvão. Molecular-dynamics simulations of carbon nanotubes as gigahertz oscillators. *Phys. Rev. Lett.*, **90**, 055504 (2003).

[9] S.B. Legoas, V.R. Coluci, S.F. Braga, P.Z. Coura, S.O. Dantas, D.S. Galvão. Gigahertz nanomechanical oscillators based on carbon nanotubes. *Nanotechnology*, **15**, S184 (2004).

[10] J.L. Rivera, C. McCabe, P.T. Cummings. The oscillatory damped behaviour of incommensurate double-walled carbon nanotubes. *Nanotechnology*, **16**, 186 (2005).

[11] P. Liu, Y.W. Zhang, C. Lu. Oscillatory behavior of gigahertz oscillators based on multiwalled carbon nanotubes. *J. Appl. Phys.*, **98**, 014301 (2005).

[12] V.R. Coluci, S.B. Legoas, M.A.M. de Aguiar, D.S. Galvão. Chaotic signature in the motion of coupled carbon nanotube oscillators. *Nanotechnology*, **16**, 583 (2005).

[13] P. Liu, Y.W. Zhang, C. Lu. Analysis of the oscillatory behavior of double-walled carbon nanotube-based oscillators. *Carbon*, **44**, 27 (2006).

[14] J.W. Kang, H.J. Hwang. Gigahertz actuator of multiwall carbon nanotube encapsulating metallic ions: molecular dynamics simulations. *J. Appl. Phys.*, **96**, 3900 (2004).

[15] Y. Kimoto, H. Mori, T. Mikami, S. Kata, Y. Nakayama, K. Higashi, Y. Hirai. Molecular dynamics study of double-walled carbon nanotubes for nano-mechanical manipulation. *Jpn. J. Appl. Phys.*, **44**, 1641 (2005).

[16] W. Guo, W. Zhong, Y. Dai, S. Li. Coupled defect-size effects on interlayer friction in multiwalled carbon nanotubes. *Phys. Rev. B*, **72**, 075409 (2005).

[17] J.W. Kang, K.O. Song, O.K. Kwon, H.J. Hwang. Carbon nanotube oscillator operated by thermal expansion of encapsulated gases. *Nanotechnology*, **16**, 2627 (2005).

[18] J.W. Kang, H.J. Hwang. Nanoscale carbon nanotube motor schematics and simulations for micro-electro-mechanical machines. *Nanotechnology*, **15**, 1633 (2004).

[19] J.J. Rivera, C. McCabe, P.T. Cummings. Oscillatory behavior of double walled nanotubes under extension: a simple nanoscale damped spring. *Nano. Lett.*, **3**, 1001 (2003).

[20] J.W. Kang, K.O. Song, H.J. Hwang, Q. Jiang. Nanotube oscillator based on a short single-walled carbon nanotube bundle. *Nanotechnology*, **17**, 2250 (2006).

[21] T. Hertel, R.E. Walkup, P. Avouris. Deformation of carbon nanotubes by surface van der Waals forces. *Phys. Rev. B*, **58**, 13870 (1998).

[22] M.H. Park, J.W. Jang, C.E. Lee, C.J. Lee. Interwall support in double-walled carbon nanotubes studied by scanning tunneling microscopy. *Appl. Phys. Lett.*, **86**, 023110 (2005).

[23] K.R. Byun, J.W. Kang, H.J. Hwang. A study on nanotube-substrate interaction effect for fullerene-shuttle-memory based on nano-peapod. *Physica. E*, **28**, 50 (2005).

[24] J.W. Kang, H.J. Hwang, J.H. Lee, H.J. Lee, O-K. Kwon, K. Lee, Y-M. Kim. Substrate-induced structural deformations of fullerene-shuttle memory device. *J. Korean Phys. Soc.*, **47**, S552 (2005).

[25] J. Tersoff. Empirical interatomic potential for silicon with improved elastic properties. *Phys. Rev. B*, **38**, 9902 (1988).

[26] J. Tersoff. Modeling solid-state chemistry: interatomic potentials for multicomponent systems. *Phys. Rev. B*, **39**, 5566 (1989).

[27] D.W. Brenner. Empirical potential for hydrocarbons for use in simulating the chemical vapor deposition of diamond films. *Phys. Rev. B*, **42**, 9458 (1990).

[28] H. Ulbricht, G. Moos, T. Hertel. Interaction of C_{60} with carbon nanotubes and graphite. *Phys. Rev. Lett.*, **90**, 095501 (2003).

[29] S. Arcidiacono, J.H. Walther, D. Poulikakos, D. Passerone, P. Koumoutsakos. Solidification of gold nanoparticles in carbon nanotubes. *Phys. Rev. Lett.*, **94**, 105502 (2005).

[30] P.M. Agrawal, B.M. Rice, D.L. Thompson. Predicting trends in rate parameters for self-diffusion on FCC metal surfaces. *Surf. Sci.*, **515**, 21 (2002).

[31] J.W. Kang, H.J. Hwang. An ultrathin carbon nanoribbon study as a component of nanoelectromechanical devices. *Mol. Simul.*, **31**, 561 (2005).

[32] J.W. Kang, H.J. Hwang. Molecular dynamics simulations of Single-Wall GaN Nanotubes. *Mol. Simul.*, **30**, 29 (2004).

[33] J.W. Kang, H.J. Hwang. Fullerene nano ball bearings: an atomistic study. *Nanotechnology*, **15**, 614 (2004).

[34] J.W. Kang, H.J. Hwang. The electroemission of endo-fullerenes from a nanotube. *Nanotechnology*, **15**, 1825 (2004).

[35] J.W. Kang, H.J. Hwang. Model schematics of a nanoelectronic device based on multi-endo-fullerenes electromigration. *Physica. E*, **27**, 245 (2005).

[36] Y.Q. Xue, S. Datta. Fermi-level alignment at metal carbon nanotube interface: application to scanning tunneling spectroscopy. *Phys. Rev. Lett.*, **83**, 4844 (1999).